



Cyanides, Arsenic, and Noble Metals in Abandoned Gold Ore Cyanidation Tailings and Surface Waters in a Permafrost Region (Transbaikal Territory, Russia)

Nataliya Yurkevich^{1,2} · Vladimir Olenchenko¹ · Svetlana Bortnikova¹ · Olga Saeva¹ · Tatyana Korneeva¹

Received: 4 September 2020 / Accepted: 11 September 2021 / Published online: 23 September 2021
© Springer-Verlag GmbH Germany, part of Springer Nature 2021

Abstract

Geochemical and geophysical investigations were performed in an area of the Darasun ore cyanidation tailings impoundment, which is located in a permafrost region. The tailings contain up to 40 wt% pyrite and 5.7 wt% arsenopyrite. The purpose of this work was to determine the composition and mechanisms of transformation of the tailings and species of As, Au, Ag, Be, and Tl in drainage waters and the Darasun River before and after mixing with technogenic flows from the mining area. When the waste is oxidized because of the repeated seasonal freezing and thawing of water, three groups of chemical elements are leached: typical ore metals and impurity elements (Pb–Co–Ni–Zn–Cd and Fe–Al–Ti–Be–In), noble metals, metalloids (Au–Ag–Cu–As–Sb–Se), and post-transition metals and metalloids (Bi–Sn–Te). Drainage waters with salinities up to 5 g/L form, with concentrations of sulfate ions up to 2 g/L and cyanide up to 4 g/L, high concentrations of Au (up to 130 µg/L), Ag (3.8 µg/L), As (up to 350 µg/L), and Sb (up to 1100 µg/L), and impurity elements (Tl, In, Be, and Bi). The drainage water flows into the Darasun River, resulting in hydrochemical anomalies tens of kilometers downstream.

Keywords Mine tailings · Electrical resistivity tomography · Cryogenic leaching · Drainage · Mobility · Geochemical barrier

Introduction

Sulfide-containing mine wastes can be a source of acidic drainage, which often contains high concentrations of As, Pb, Hg, Cd, Cr, and other metals, as well as sulfate and

cyanide ions (Bortnikova et al. 2019; Dold and Fontboté 2001; Hudson-Edwards et al. 2011; Luque-Almagro et al. 2016; Nordstrom 2011; Nordstrom et al. 2015; Saryg-ool et al. 2017; Sinclair et al. 2015; Woffenden et al. 2008; Yurkevich et al. 2012, 2015, 2019). The leaching of contaminants from gold mining waste storage areas is an actively researched topic (Albert et al. 2017; Baena et al. 2020; Carvalho et al. 2017; Lortzie et al. 2015; Njinga and Tshivhase 2017). Albert et al. (2017) reported that extensive changes in river course, water, and sediment quality have occurred downstream of a gold mine (Solomon Islands) since its development: ≈ 0.087 mg/L of As is present in the water and 377 mg/kg of As is present in the sediment. The mine wastes of an old gold mining area (Escádia Grande, Portugal) contain ≈ 8090 mg/kg As and 70.1 mg/kg Sb. The waters of the stream that cross the mining area had concentrations of As up to 284 µg/L. The use of river beaches for recreational purposes increases the potential cancer risk, mainly due to As exposure (Carvalho et al. 2017). The tailings of abandoned gold–silver enrichment plants (Mitsero, Cyprus) contain high levels of cyanide (≈ 45.85 mg/kg) and leachable Cu, Fe, Zn, Cr, Pb, and Mn concentrations (Lortzie et al. 2015).

✉ Nataliya Yurkevich
yurkevichnv@ipgg.sbras.ru

Vladimir Olenchenko
olenchenkovv@ipgg.sbras.ru

Svetlana Bortnikova
bortnikovasb@ipgg.sbras.ru

Olga Saeva
saevaop@ipgg.sbras.ru

Tatyana Korneeva
korneevatv@ipgg.sbras.ru

¹ Trofimuk Institute of Petroleum Geology and Geophysics, Siberian Branch of the Russian Academy of Sciences, Novosibirsk, Russia

² Novosibirsk State University, Pirogova str. 2, 630090 Novosibirsk, Russia

Oxidation of the wastes of the ore cyanide process (Ursk, Kemerovo region, Russia) produces acidic drainage water with high concentrations of sulfate, Fe, Al, Cu, Zn, Pb, As, Se, Te, Hg, Cd, and REEs, which flow into the Ur River. The stream also transports gold and silver as dissolved, colloidal, and particulate forms (Myagkaya et al. 2016).

Gold mining wastes associated with cyanide leaching pose a serious environmental hazard. Most of the placer and indigenous gold deposits in Russia are located in areas with cold climatic conditions, including the Urals, Siberia, and the Far East (Laperdina 2002). Previously, it was believed that cyanide leaching was not a problem in permafrost conditions since the waste would freeze and thus be partially removed from interaction with environmental components, thereby reducing adverse environmental consequences. The frozen rocks were considered a zone of "zero chemistry." However, it was found that permafrost is not geochemically isolated (Allan and Hornbrook 1970; Williams 1964) and frozen waste is still subject to a combination of physical and chemical processes, and pore solutions continue to migrate at low temperatures.

Thus, gold ore cyanidation wastes in such areas may still undergo active hyper-cryogenic transformations during the repeated seasonal freezing and thawing of water and intensive oxidation. Potentially toxic compounds can enter river systems from dumps and tailings dumps that are accessible to water and wind and vegetation. There are numerous examples of abandoned old tailings in Siberia that pollute the water, air, and soil (Bortnikova et al. 2018, 2019). Problems with environmental pollution in such waste areas have been reported by researchers in Canada (Davé and Blanchette 1999; Little et al. 2020; Mudroch and Clair 1986) and the USA (Khamkhash et al. 2017; Straskraba and Moran 1990). Davé and Blanchette (1999) reported that even at low temperatures, acid production does not stop completely, although it does slow down. Thus, this problem is relevant for the cold regions of the USA, China, Russia, and Canada.

To understand the transformations of a sulfide-containing substance under the influence of such seasonal temperature fluctuations, especially in the seasonal thaw layer, it was necessary to study the chemical composition of the waste as well as the relationship between the waste and surface watercourses to determine the mobility of elements in the wastewater system and predict the further flow of chemical compounds into natural watercourses. Such studies are particularly relevant since gold mining waste is a source of cyanide anions and elements of hazard class 1 (As, Tl, Be), which have high mobility and toxicity.

One of the methods used to describe the structure of a man-made system is electrical resistivity tomography (ERT). The use of ERT enables the identification of water structures in the body of the dump, allowing us to contour the filtration channels of underground drainage and show its seepage

into the groundwater horizon (Acosta et al. 2014; Gabaron et al. 2020; Martín-Crespo et al. 2020; Nikonow et al. 2019; Olenchenko et al. 2016). ERT has been used in many applications to delineate frozen and unfrozen areas of the subsurface (Hayley et al. 2007; Kneisel et al. 2014; Krautblatter et al. 2010; Oldenborger and LeBlanc 2018). Herring et al. (2019) provided insight into the physical mechanisms that govern the resistivity of porous media at sub-zero temperatures and provided a starting point for the quantitative analysis of resistivity data collected in frozen ground. ERT has been used to determine degrees of salinity in frozen rock (Kvon et al. 2019), while Gao et al. (2019) demonstrated the capability of ERT to delineate the distribution of aquifers in supra- and sub-permafrost waters.

The use of micro-ERT in combination with geochemical testing data enables the study of the near-surface space of the portion of the waste that is located within the seasonal thaw layer and undergoes the greatest transformations due to the freezing and thawing of water, which results in oxidation (0–1.5 m) (Epov et al. 2017; Yurkevich et al. 2017). Using ERT, it is possible to determine the most oxidized, washed, and decompressed sands that have undergone the greatest leaching and removal of elements (zones with a relatively higher resistance). At the same time, areas with low resistances correspond to the dense wet tailings that are least susceptible to oxidation and contain the highest concentrations of dissolved contaminants.

Hyper-cryogenic transformation of sulfide-containing gold mining waste, as well as the features of technogenic dispersion of noble metals and trace element-impurities have been insufficiently studied in permafrost areas. The purpose of this work was to determine: (1) the composition and transformation mechanisms of gold mining sulfide-containing wastes after ore cyanidation and (2) the composition and species of As, Au, Ag, Be, and Tl in associated drainage waters and waters of the Darasun River before and after mixing with technogenic flows in the mining area.

Study Area

The study area includes the sulfide-containing wastes of the Darasun gold mine and surface watercourses that are subject to anthropogenic impact from the mining infrastructure of the Darasun ore cluster (Transbaikal region, Vershinno-Darasun village, Fig. 1). In Soviet times, the Darasun mine was the second most important gold mining enterprise in the Chita region. Approximately 100 t of Au are now on the mine's balance sheet, with the main reserves concentrated mainly in the Darasun deposit, which is characterized by an abundance of carbonate minerals and has a specific feature: all ore veins of the deposit are localized exclusively among igneous rocks. The main ore minerals are pyrite,



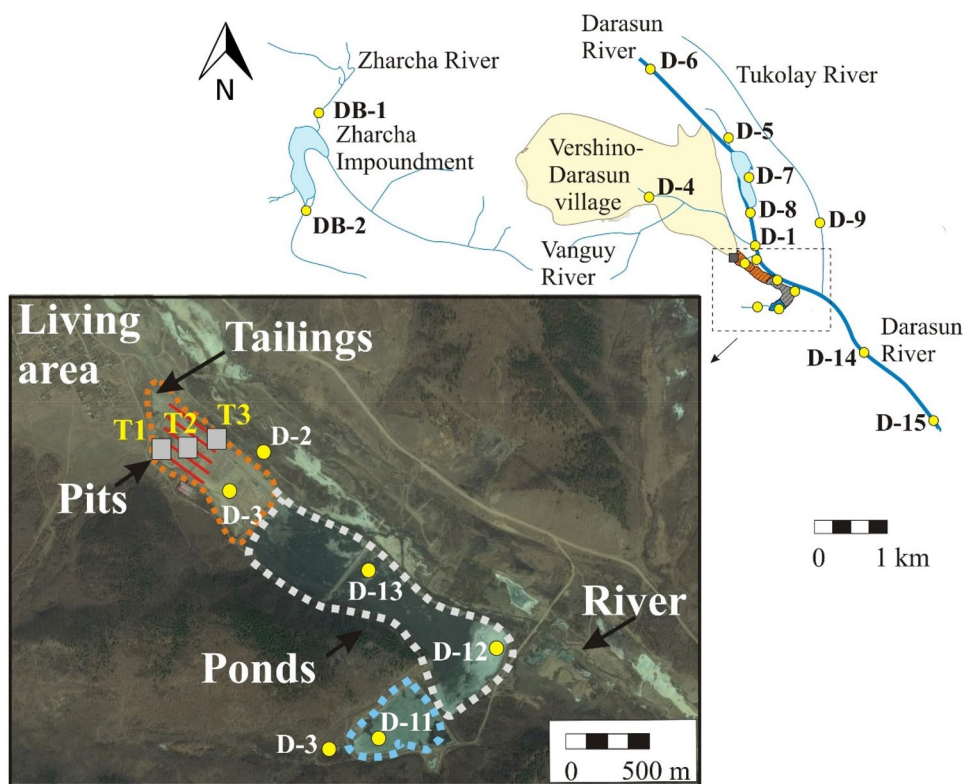
Fig. 1 Map of the Transbaikal region and the study area location

arsenopyrite, chalcopyrite, pyrrhotite, tennantite, sphalerite, galena, Cu, Ag, As, Bi, and Pb sulfosalts (sulfides account for 40–60%), Bi, and Te minerals, and native Au. Vein minerals include quartz, tourmaline, carbonates, gypsum, and anhydrite and the ores contain a large amount of arsenopyrite. The host ores are characterized by high levels of Au and Ag, as well as Cu, As, Sb, Bi, Pb, and Te. The main carriers of gold are arsenopyrite, pyrite, chalcopyrite, pyrrhotite, and tennantite.

Currently, there are three types of mine wastes stored in the Darasunsky ore cluster: oxidizing roasting cinder of the arsenopyrite ores (50,000 t), cyanide cakes (100,000 t), and flotation tailings ($\approx 4,700,000$ t). Wastes are located a short distance from residential buildings, bordering the tailings dump of the Darasun processing plant and the channel of the Darasun River (Fig. 2).

The flotation and cyanidation tailings of gold ore processing are stored in dumps and hydraulic dumps at the border of Vershino-Darasun village (Tugokochensky district of the Transbaikal Territory). In addition, there are workings of artisanal miners. In the southern part of the study area, the hydraulic dumps contain liquid cyanidation wastes and associated effluents. Local streams and the Darasun River flow below the dump. Ore processing is currently handled by the Darasun processing plant, which supplies pulp with industrial waste to the hydraulic dump. Waste cyanide cinder from private production was received at the same site after 2010. During the fieldwork, the Darasun River was sampled

Fig. 2 Locations of sample points and satellite images of the Darasun mine tailings area. Yellow circles—water sampling points D-1 ÷ D-15, DB-1, and DB-2; gray squares—pits T1, T2, and T3



upstream and downstream of the tailings, along with background sampling points of the Zharcha River and Zharcha reservoir. ERT studies were performed on a selected site at the old tailings dump.

Methods

Field Study

During the field and laboratory work, the Darasun mine tailings area was investigated using geochemical sampling and a geophysical survey.

Sampling

To determine the composition of the solid tailings, the Darasun tailings were sampled at three 100–120 cm deep pits (gray squares, pits T1, T2, T3, Fig. 2). In total, thirty 200 g samples were collected using a plastic scoop and transferred into polyethylene bags for chemical analysis.

Fifteen 1 L water samples were collected at each sampling point (Fig. 2) at a depth of ≈ 10 cm. Sample sites included the: Darasun River near the tailings (D-1); drainage stream, upstream (D-2) and downstream (D-3) of the small gravity separation plant; the technological pond near the Darasun processing plant in the living area (D-4); spring flowing into Baikalskoe Lake to the south of the village (D-5); groundwater from a drinking water well (D-6); Baikalskoe Lake (D-7); creek downstream of the lake (D-8); Tukolay River (D-9); natural spring behind the dam of settling Pond 1 in the southern part (D-10); settling Pond 2 near the dam (D-11); settling Pond 1 (D-12); fresh pulp entering Pond 1 (D-13); Darasun River below the dumps (D-14); and Darasun River near the Nizhny Stan village (D-15).

To evaluate the background, we sampled the Zharcha River (DB-1) and the Zharcha Reservoir, which is used for drinking and commercial purposes (DB-2). These are both located 5 km from the waste disposal area (Fig. 2). The samples were collected in plastic bottles that were rinsed with the sampled water.

Field Measurements

The pH and redox potential (Eh) of the water samples were measured in situ using a pH/°C meter (HI 9025 C, Hanna Instruments, Italy), with a combined glass electrode for pH (HI 1230 B, Hanna Instruments), and a Pt electrode for Eh (oxidation reduction potential electrode, Hanna Instruments) (Nordstrom 2011). Electrical conductivity (EC) was determined using a conductivity meter Cond 315 i (WTW, USA).

The solid samples were mixed with distilled water at a “water/solid” ratio of 1/2 by mass to prepare pastes

according to Sobek et al. (1978). The pH, redox potential (Eh), and EC were measured in situ.

The water samples were divided into two sets. The first 50 mL aliquot was filtered at the sampling site to $< 0.25 \mu\text{m}$ using a microfiltration hydrophobic membrane (Vladipor, Russia) and acidified with distilled HNO_3 (purity 99%) to $\text{pH} < 2$. The second one, intended for anion analyses, was not filtered. The samples were transported to the laboratory and stored at $< 4 \text{ }^\circ\text{C}$.

Electrical Resistivity Tomography Survey

The ERT survey was carried out using a multielectrode resistivity meter (Skala-48, IPGG SB RAS, Novosibirsk, Russia) in five profiles to reveal the geoelectric structure of the local area to a depth of 20 m (Figs. 2, 3). The profiles were 115 m long; the distance between the electrodes was 5 m. The ERT was performed using a Schlumberger array. Additionally, the microscale profile was 14 m in length, and the distance between the electrodes was 30 cm. This configuration enabled the allocation of layers that were 15 cm thick. Data processing was performed using Res2Dinv and Res3Dinv software (Loke 2003). Two-dimensional geoelectric sections of the resistivity distribution in the area were constructed using the data processing results.

Laboratory Analysis

The solid samples were dried at room temperature for 48 h, homogenized by mixing, sieved using a 250- μm nylon filter (Fritsch, Idar-Oberstein, Germany), and powdered to $< 74 \mu\text{m}$ by abrasion in an agate mortar for bulk analysis. ICP-MS was used to determine their elemental compositions

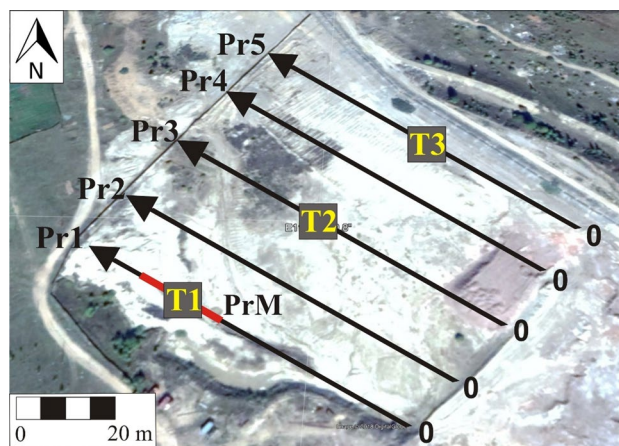


Fig. 3 Locations of the electrical resistivity profiles on the surface of the Darasun mine tailings. Black arrows Pr1–Pr5—long ERT profiles (115 m), red line PrM—microscale profile (14 m), gray squares—pits T1, T2, T3

(ELAN-9000 DRC-e, PerkinElmer Instruments LLC, USA) at the “Plasma” Analytical Centre (Tomsk, Russia). High-purity Ar (99.95%) was used as the plasma-forming, transporting, and cooling gas. A 2% solution of ^7Li , ^{59}Co , ^{89}Y , and ^{205}Tl , with a concentration of 1 g/L for each determined element (Tuning Solution, USA), was used for the adjustment. All measurements were conducted in three replicates ($n=3$) for each element. The relative standard deviation did not exceed 13% in all measurements. The relative error of the analysis was 3–8%.

In water samples, major cation (Al, Fe, Ca, Mg, K, Na, and Si) and trace element analyses were carried out using ICP-MS (ELAN-9000 DRC-e, PerkinElmer Instruments LLC, USA) at the Analytical Centre “Plasma” (Tomsk, Russia). The relative error of the analysis was estimated to be 2–5% at the mg/L concentration level and 4–8% at the $\mu\text{g/L}$ concentration level.

Another aliquot was analyzed for major anions (CN^- , SO_4^{2-} , Cl^- , HCO_3^-) using potentiometry and photometric and titrimetric methods. Accuracy and precision were estimated to be 7% or better at mg/L concentrations.

The concentrations of bicarbonate ions in the samples were determined using the titrimetric method. This definition is based on the interaction of HCO_3^- ions from the strong acid with the formation of weak carbonic acid, which is dissociated into H_2O and CO_2 in solution. Accuracy and precision were estimated to be at 10% or better at the mg/L concentration level.

The chloride concentrations in the water samples were determined using the titrimetric method with silver nitrate based on the formation of insoluble silver chloride. The accuracy and precision were estimated to be 10% or better at the mg/L concentration level.

The concentrations of cyanide ions in aqueous solutions were measured using the potentiometric method. The accuracy and precision were estimated to be 10% or better at the mg/L concentration level.

Species of the elements in the solution and the ability of water to remove them from the solution to form independent solid phases were considered using the software packages Visual Minteq 3.1 (Gustafsson 2014) and WateQ4F (Ball and Nordstrom 1991).

Results

Geophysical Survey

The ERT data indicated the layered alternation of EC: a conductive horizon to a depth of ≈ 0.5 m (green–blue, supplemental Fig. S-1), followed by a highly resistive horizon (150–300 $\Omega\cdot\text{m}$) to a depth of 3–5 m (yellow–red, Fig. S-1), a deeper conductive medium (1–30 $\Omega\cdot\text{m}$) to a depth of \approx

15 m (green–blue, Fig. S-1), and a high-resistance medium (up to 300 $\Omega\cdot\text{m}$) (red and dark-red, Fig. S-1).

The upper moderately conductive layer from the surface of the tailings to a depth of 1.4 m was interpreted as a seasonally flooded melt layer of technogenic sands that stretched to a depth of ≈ 4 m, i.e. the horizon of seasonal freezing. Thawed, moderately flooded tailings were located at depths of 4–15 m. We assumed that this was a zone of oxidation and thawing. From a depth of 15 m, it was interpreted to be solid bedrock.

Tailings Composition

The main mineral phases present in the tailings were mica, Fe–Mg chlorite, smectite, and quartz. The ore waste minerals include sulfides, sulfates, oxides, and hydroxides of Fe, Pb, Zn, and Cu. In the cyanide cakes, the proportion of sulfides was $\approx 46\%$ wt., of which pyrite accounts for 86% wt. Arsenopyrite was present to a lesser extent: 5.7%. The mass fractions of chalcopyrite, galena, and sphalerite were 0.3%, 0.2%, and 0.1%, respectively.

The tailings are fine-grained sands and the distribution of the average particle diameter indicates the heterogeneity of the material with depth: particles with a diameter of 86–300 μm prevail at depths of 0–65 cm, and finer particles, 16–28 μm , lie deeper. The pH of the pastes was distributed relatively uniformly over the entire depth of the pit: from 7.08 to 8.50, and the medium was oxidizing (Eh ranging from 350 to 444 mV), except for the horizon at a depth of 73 cm, which is characterized by a decline in Eh to 191 mV. The EC of the tailings ranged from 90 at the surface to 1818 $\mu\text{Sm/cm}$ at the deepest point of the pit (113 cm). The moisture content of the tailings ranged from 5.1% in the uppermost horizon to 30% at a depth of 73 cm (Table 1).

Among the rock-forming elements, Si, Al, and Fe prevail; the concentrations of all elements (Si, Al, Fe, Na, K, Mg, Ti, P) exceed the Clarke concentrations for the Earth's crust (Table 1). The concentrations of P, Mg, K, Al, and Fe in the medium-grained sands at depths of 0–65 cm are less than those in the deeper horizons. The upper medium-grained sands were more enriched in Si, Na, and Ti.

The concentrations of a range of trace elements exceeded the Clarke values (supplemental Table S-1), but anomalies for As (1400 times), Sb (200 times), Bi (1700 times), Ag (57 times), and Au (387 times) were especially pronounced. The greatest accumulation of these elements was typically in the horizons with a predominance of fine-grained particles at depths of 67–113 cm; the same layers are the zones with the lowest resistance of the medium in geoelectric sections (Table S-1).

Table 1 Physicochemical parameters and major element composition (in weight percent oxide) of the Darasun tailings (pit T1, samples T1-1–T1-9, different depths) and the comparison with the upper continental crust composition

Parameter	T1-1	T1-2	T1-3	T1-4	T1-5	T1-6	T1-7	T1-8	T1-9	Average in the upper continental crust ^a
Depth, cm	0–10	11–53	54–65	66–68	69–73	74–83	84–106	107–113	114–140	
pH pastes	8.50	8.18	7.86	7.19	7.23	7.08	7.17	7.17	7.21	
Eh paste, mV	350	369	414	437	389	191	430	444	442	
EC, $\mu\text{Sm/cm}$	90	98	288	881	1503	1650	1400	1521	1818	
Humidity, %	5.1	10	10	20	27	30	29	23	25	
Grain size, μm	300	202	154	86	24	16	22	28	20	
SiO ₂	62	65	64	62	51	51	51	53	40	67
Al ₂ O ₃	31	27	28	27	34	34	33	33	29	15
FeO	8.4	7.6	7.3	8.0	9.0	8.7	8.6	9.1	9.9	5.0
Na ₂ O	7.9	4.6	4.5	4.5	3.0	2.9	3.2	3.2	3.0	3.3
K ₂ O	6.0	4.8	4.0	4.3	6.2	6.1	5.6	4.8	5.5	2.8
MgO	2.7	2.2	2.3	2.4	2.9	3.0	3.1	3.6	4.1	2.5
TiO ₂	0.90	1.0	1.0	0.94	0.86	0.92	0.83	0.89	0.94	0.64
P ₂ O ₅	0.38	0.38	0.42	0.51	0.57	0.58	0.59	0.55	0.59	0.15

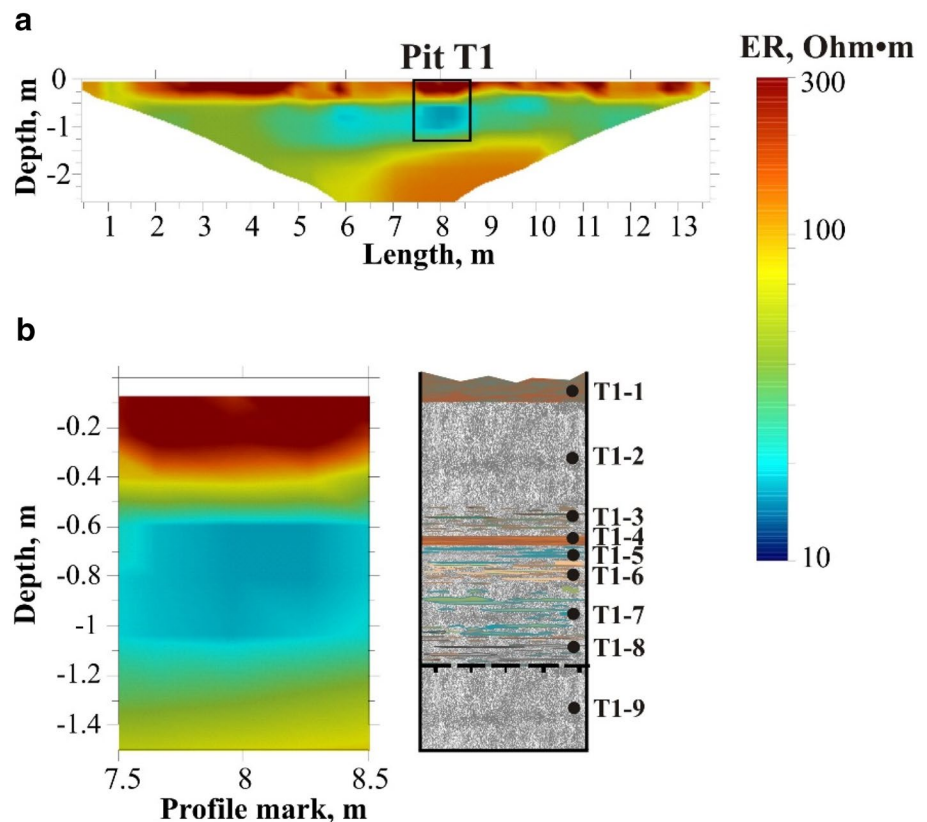
^aRudnick and Gao (2003)

Comparison of the Geophysical Data and Geochemical Composition of the Tailings

A geoelectric section, constructed according to the micro-ERT profile, gives an idea of how layers with different ECs

alternate (Fig. 4a). A fragment of the geoelectric section (Fig. 4b) was compared with the geochemical testing data of a pit from the depth of the seasonally thawed layer to frozen rocks (the depth of seasonal freezing is 1.4 m) to verify the resistivity with the chemical composition (Table 1).

Fig. 4 Geoelectric section according to the profile of micro-ERT tomography (a), comparison of a fragment of the geoelectrical section (b on the left) with a description of the pit (b on the right)



The uppermost layers are at a depth of 53 cm in the zone of active cryogenic transformation, and this zone has undergone intensive weathering due to seasonal fluctuations in temperature and humidity; a wide range of contaminants are leached and removed with water flows. Such layers are characterized by larger particle sizes, less humidity (5–10%) than other horizons, low EC and redox potential (Table 1, samples D-1, D-2), and relatively low element concentrations compared to the underlying fine-grained material (Table S-1, samples D-1, D-2); these zones are marked on the geoelectric sections as relatively high resistance zones (Fig. 4b).

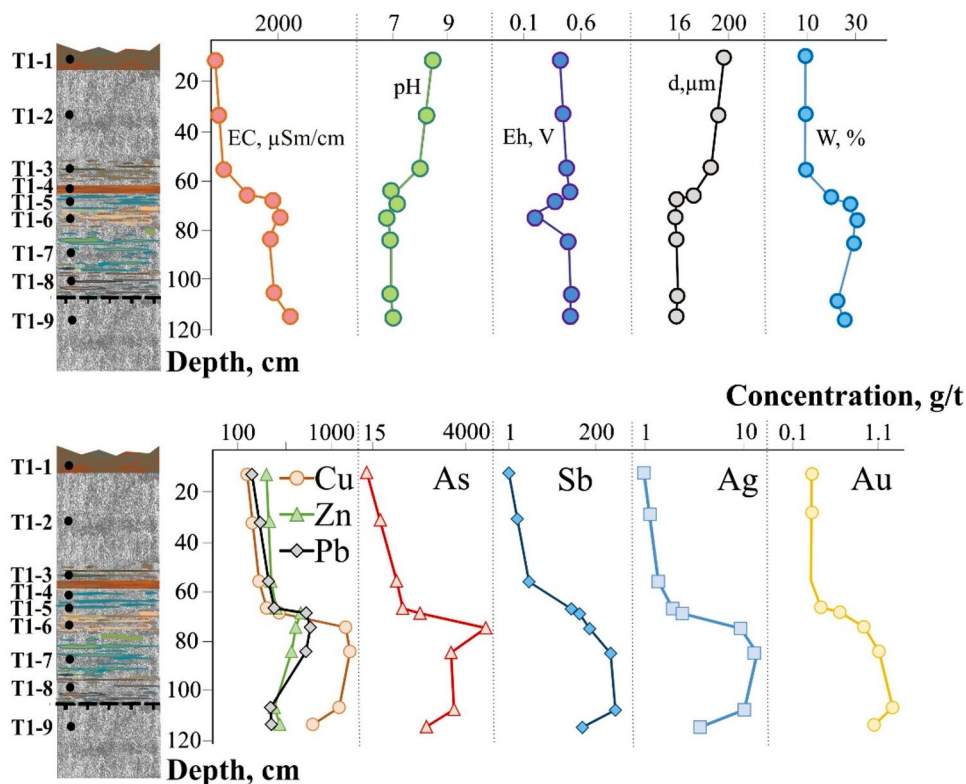
In the intermediate horizon, at a depth of 50–113 cm, the moist fine-grained material (humidity 25–30%) had increased redox potentials, in which As (up to 4831 g/t), Se (up to 6.1 g/t), Sb (up to 170 g/t), Au (up to 1.1 g/t), Ag (up to 7.7 g/t), and a wide range of elements of the ore association were present at high concentrations. This horizon, though protected from direct sunlight, is periodically leached by water and dries out, being within the seasonal melt layer. Thus, it undergoes cryogenic changes under the influence of temperature fluctuations. Here, the substance may seem to be unaffected; however, it undergoes oxidation (as evidenced by the high Eh) and the formation of mobile chemical complexes in pore solutions and can be transported by capillary uplift and underground drainage seepage. Such horizons correspond to zones of reduced resistance in the ERT geoelectric sections (Fig. 4). Over

time, these layers, by analogy with the overlying layers, will undergo oxidation, weathering, and the removal of chemical elements with water flow. A physicochemical geochemical barrier was discovered at a depth of 65–70 cm with a sharp increase in the Eh value (Fig. 5) and concentrations of total dissolved solids within this layer.

Another geochemical barrier concentrating chemical elements was identified at a depth of 113 cm at the border with frozen soil. Horizons deeper than 1.13 m are represented by frozen soils, a zone of relatively low reactivity with low rates of chemical reactions, which is reflected in the reduced EC of the medium. The active layer is traced to an accuracy of 5 cm by micro-electrotomography, which allows the further use of ET to contour the leaching horizons and concentration of the substance. Such dusty sands with high redox potentials and concentrations of chemical elements were assumed to correspond to conducting zones at a depth of 4–15 m (Fig. 4) below the seasonal freezing horizon.

Based on a combined analysis of geophysical and geochemical data, it could be concluded that the zone of active hypergene weathering and water leaching exists on the surface of the waste to a depth of 50 cm, where leached disintegrated medium-grained sands were located. Then, a moist, dense, dusty layer was found, in which the sulfide minerals were concentrated (to depths of 1.4 m). These are subject to oxidation during cryogenic processes.

Fig. 5 Distribution of physico-chemical parameters and chemical elements in the tailings samples (pit T1) with pit depth



Water Samples Composition

Water in surface drainage streams (samples D-1 and D-4) had a neutral pH (7.4), mineralization of 1–1.2 g/L, and a predominance of sulfate anions over chloride and bicarbonate anions (supplemental Table S-2). In the old dump, the concentration of cyanide anions was 4 g/L, which explains the high percentage of CN⁻ (65%) among the anions (sample D-11, supplemental Table S-2). The drained pulp samples contained 700 mg/L CN⁻ (44%). The cationic composition of the drainage streams was dominated by Ca and Mg, except at the old dump (sample D-11), where the main anion was Na (91%). After the Darasun River mixed with the drainage streams, the solutions were neutral, mineralization was 0.8 g/L, and sulfate (78%) and bicarbonate (18%) anions predominated.

A wide range of trace elements was found in the water leaching from the tailings. These elements included a group

of typical ore components (Fe, Cu, Zn, Cd, Pb), impurities (As, Sb, Be, Tl), and noble metals (Ag, Au) (Table 2).

To better understand the mechanisms of element migration, the chemical species in the solution were calculated. Typical ore metals (Cu, Zn, Cd, Pb) behave differently at the background point (DB-1) and have minimal technogenic influence. The main forms of Zn and Cd are in the form of free cations with an oxidation state of 2⁺ (Zn²⁺, Cd²⁺) with a certain amount of carbonate and sulfate forms. Pb and Cu are present here mainly in the form of carbonate complexes PbCO₃(aq) (65%), PbHCO₃⁺ (11%), and CuCO₃(aq) (81%). Thallium in the background water is predominantly the free Tl⁺ cation (99.4%). Beryllium, on the other hand, demonstrates the typical properties of the complexing agent; its main form in natural water is Be(OH)₂(aq) (99.9%), and the remaining 0.1% is Be²⁺ and BeCO₃(aq) (supplemental Fig. S-2).

Table 2 Concentrations of trace elements in the surface waters of the Darasun mine tailings area

Parameter	Mine drainage				RBDD						Technological ponds			RADD		Background	
	D-1	D-2	D-3	D-4	D-5	D-6	D-7	D-8	D-9	D-10	D-11	D-12	D-13	D-14	D-15	DB-1	DB-2
As	83	8.6	240	6.9	37	1.3	11	71	88	22	350	4.5	3.9	65	27	1.1	1.9
P	57	1.0	8.8	1.0	20	1.3	31	22	8	31	8.0	1.0	1.0	23	1.0	3.2	6.3
Sb	37	25	26	18	9.1	0.27	1.4	1.6	10	1.0	1100	10	6.3	18	7.5	1.1	0.36
Zn	31	7500	12,000	350	8.7	5.2	10	8.1	14	11	16	37	24	23	25	6.4	5.9
Cu	22	9300	13,000	23	12	2.2	6.6	11	30	7.9	230,000	190	370	500	710	2.3	3.0
Ba	16	34	5.3	8.2	19	14	19	26	42	26	0.50	29	32	68	7	11	5.0
Pb	7.7	32	6.8	4.2	1.6	1.8	4.1	1.3	6.4	1.6	1.8	4.6	2.5	2.6	3.0	1.3	1.2
Ni	7.0	260	330	24	1.7	0.74	2.0	3.1	4.5	1.8	150	15	8.8	18	7.1	1.4	1.2
Li	5.0	280	500	14	2.4	3.6	2.0	2.3	4.0	8.5	4.6	27	26	14	10	4.0	1.8
Ti	3.9	2.8	4.6	2.2	1.4	1.2	0.85	0.67	1.4	0.50	1.2	1.9	7.0	0.97	2.1	0.99	0.93
Rb	2.4	6.5	15	15	1.0	0.75	1.4	1.2	1.2	1.4	3.0	48	55	8.8	4.3	0.56	1.2
Co	2.0	190	250	21	0.20	0.15	0.26	0.26	2.2	0.22	150	4.9	2.3	20	6.8	0.11	0.089
Mo	1.1	0.56	0.20	2.1	0.88	1.0	0.88	1.5	3.1	0.50	95	22	23	7.1	2.9	0.49	1.2
Cr	0.56	1.1	2.5	0.19	0.34	0.18	0.29	0.34	0.32	0.28	2.5	0.25	0.21	0.30	0.10	0.25	0.26
V	0.52	0.27	1.0	0.05	0.60	0.46	0.85	0.99	0.46	0.21	1.8	0.05	1.4	2.0	0.53	0.16	0.29
Cd	0.33	59	100	3	0.19	0.11	0.15	0.13	0.19	0.18	0.32	0.32	0.20	0.27	0.88	0.17	0.10
Bi	230	82	95	53	29	14	25	68	4700	24	10	10	33	10	10	12	11
Te	160	5.0	120	5.0	35	5.0	36	31	3000	18	32	27	29	67	5.0	5.0	11
Ag	140	83	510	50	10	10	10	10	18	11	3800	10	100	20	18	12	10
W	130	71	110	150	23	14	38	12	360	18	26,000	2200	5200	220	50	11	15
Se	50	50	3400	740	180	50	270	63	420	91	32,000	1100	44	50	50	50	14
Sn	50	69	28	6.8	43	35	30	74	170	120	140	61	61	150	52	41	35
Tl	42	140	250	130	6.5	4.0	5.1	10	65	6.7	1.0	160	39	87	42	7.3	3.1
Au	31	13	65	1600	5.1	5.0	5.0	5.0	5.0	24	130,000	32,000	6000	7100	2300	5.0	5.0
In	5.8	5.0	12	5.0	5.0	5.0	5.0	5.0	5.7	5.0	5.0	5.0	5.0	5.0	5.0	5.0	5.0
Be	5.0	860	1400	5.0	5.0	5.0	7.6	10	5.0	6.8	5.0	5.0	5.0	17	21	5.6	13

The concentrations of As ÷ Cd are in µg/L; Bi ÷ Be are in ng/L. D-1 ÷ DB-2—the names of the water samples (Fig. 2) RBDD Darasun River before drainage discharge, RADD River after drainage discharge

In acidic mine drainage (sample D-3, pH 3.6), the proportion of thallium sulfate complexes increased to 11%, and the remaining 89% was present as free Tl⁺ cations. For the Cu, Zn, and Cd, ≈ 65% were free cations, and the remaining 35% were sulfate complexes MeSO₄(aq) and Me(SO₄)₂²⁻. Silver also exhibited typical cationic properties, with Ag⁺ accounting for 59% of all its forms, AgCl(aq) chloride complexes accounting for 31%, AgSO₄⁻ sulfate complexes accounting for only 5.5%, and Ag(CN)²⁻ cyanides were 4.5%. Only the Pb in sample D-3 was characterized by a predominance of sulfate complexes over other forms (52%), which was explained by the low solubility of lead sulfate. For the complexing ions, Be²⁺ and Au³⁺ behaved differently in acidic sulfate solutions. The proportion of free Be²⁺ cations was 77%, with only 23% represented by the sulfate complexes, BeSO₄(aq) and Be(SO₄)₂²⁻. In contrast, the proportion of the free cation Au³⁺ in acidic drainage waters accounted for only 1%. The dissolved gold was predominantly hydroxide complexes, Au(OH)₄⁻ (68%) and AuOH²⁺ (31%) (supplemental Fig. S-2).

In the subalkaline waters of the old hydraulic dump, with its high content of cyanides (D-11), the main forms of Zn, Cd, and Ag were cyanide complexes. Pb was present as carbonate complexes Pb(CO₃)₂²⁻ (29%), PbCO₃ (aq) (66%), and hydroxide PbOH⁺ (5%). Cu was represented by hydroxides Cu₃(OH)₄²⁺ (48%), carbonates CuCO₃(aq) (34%), and Cu(CO₃)₂²⁻ (16%). The predominant form of Au was the hydroxide complex Au(OH)₄⁻ (Fig. S-2).

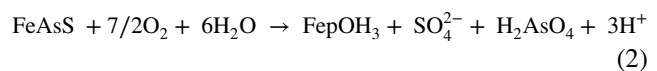
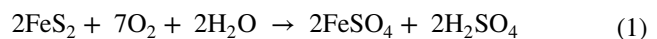
Free Cd²⁺ and Zn²⁺ cations predominated (70–75%) in the Darasun River downstream after the mine tailings area (D-15), but the sulfate complexes in the overall balance were significantly more than those at the background point (18% vs. 3%). The proportion of free Pb²⁺ and Cu²⁺ cations, as well as their sulfate complexes, was 10% higher than in the background samples, and carbonates and bicarbonates were, in contrast, 20% lower, but they constituted the bulk of all of the Pb and Cu. Similarly, the proportion of sulfate complexes in the waste of TISO₄⁻ increased to 5% (compared to 0.6% in the background river), although its main form was the free Tl⁺ cation (95%). For Be, the proportion of its sulfate complexes was insignificant (0.01%), and Be²⁺ content was slightly increased (0.1%); however, Be(OH)₂(aq) was the main form, as in the background water body. Silver migrated to the Darasun River in the form of the cyanide complex Ag(CN)²⁻, and Au⁻ migrated in the form of the hydroxide, Au(OH)₄⁻ (Fig. S-2).

Comparing the chemical forms of the elements in the Darasun River downstream after the Darasun waste with the background Zharcha River revealed an unambiguous trend: the proportion of free cations and sulfate complexes of metals Cu, Zn, Cd, and Pb increased by ≈ 10%, and carbonate complexes decreased by 20% as a result of the technogenic impact on the watercourse. A slight increase in the fraction

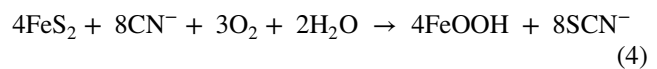
of free-cation and sulfate forms was also characteristic of Be and Tl. The noble metals Ag and Au were bound by cyanide, chloride, and hydroxo-complexes.

Discussion

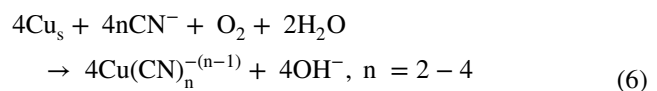
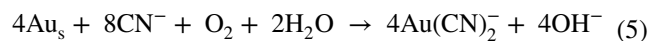
Following oxidation, sulfide minerals (mainly pyrite) are turned into dust in the seasonally thawed layer. This hypercryogenesis zone forms due to the freezing and thawing of water; the acid that forms leaches the metals and metalloids from the other now fine-grained sulfide minerals (arsenopyrite, galena, sphalerite) (Acero et al. 2007; Hawkins 2014; Parbhakar-Fox and Lottermoser 2015):



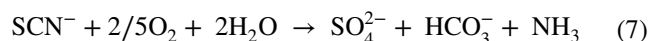
In addition, in sulfide wastes, an oxidative reaction of pyrite with residues of cyanide reagents occurred with the formation of a thiocyanate ion (Breuer et al. 2008; Parbhakar-Fox 2016):



Noble metals (Ag, Au) and Cu reacted with the cyanide anion to form mobile soluble cyanide complexes (Marsden and House 2006; Parbhakar-Fox 2016; Ghasemi et al. 2018):



Long-term interaction of the thiocyanate ion with atmospheric oxygen leads to its decomposition and the formation of sulfate, bicarbonate ions, and ammonia (U.S. EPA 1994):



A study of the material composition of the Darasun waste indicated the presence of horizons in which chemical elements were leached and removed, especially in the zone of hypercryogenesis of three groups: ore elements (Fe, Cu, Zn, Cd, and Pb), noble metals and metalloids (Au, Ag, As, and Sb) and impurity elements (Be, Tl). The first dissolved due to the oxidation of sulfide minerals (reactions 1–3). Gold and silver migrate as colloidal particles and soluble complex compounds with cyanide ligands (reaction 5). Copper can also enter solution by complexation with cyanide anions. The results of the correlation analysis confirmed such a

migration path in aqueous solutions: $KK(\text{Au}-\text{CN}^-)=0.97$, $KK(\text{Ag}-\text{CN}^-)=0.99$, and $KK(\text{Cu}-\text{CN}^-)=1$ (supplemental Table S-3).

For Tl and Be, which do not form their own sulfides in waste, there are two options: the dissolution of secondary sulfate minerals and the destruction of sulfide minerals in which they are impurities. This mechanism is supported by positive significant correlation coefficients of the concentrations of these elements and sulfate ions in solution: $KK(\text{Tl}-\text{SO}_4^{2-})=0.59$, $KK(\text{Be}-\text{SO}_4^{2-})$, and by the absence of any significant correlation between the concentrations of these elements and any other anions.

A study of the composition of surface watercourses around the stored waste showed three groups of hydrochemical anomalies, which indicated the mobility of chemical elements in the “waste—natural surface water” system (Table S-3):

1. Pb–Co–Ni–Zn–Cd–Cu–Fe–Al are typical ore metals while Tl–Be–In are impurity elements. The high correlation coefficients of these elements with pH and the concentrations of Fe, Al, Mn, and SO_4^{2-} indicate that the output of these dissolved elements was associated with sulfide oxidation, the formation of sulfate solutions, dissolution by the acidity of the medium, and sorption on Fe(III), Mn(IV), Al(III) hydroxides.
2. Au–Ag–As–Sb–Se are noble metals and metalloids, the concentrations of these in an aqueous solution are regulated by complexation with CN^- , Cl^- , and HCO_3^- anions.
3. Bi–Sn–Te are post-transition metals and metalloids, the concentrations of which correlated only with each other in the absence of significant correlations with other components, acidity, or anions. Their behaviour was controlled by the solubility of their own minerals: Bi_2Te_3 , Bi_2S_3 , SnTe, and SnS.

Studying the spatial distribution of element concentrations in the surface watercourses made it possible to identify the hydrochemical anomalies caused by anthropogenic influences. The concentrations of chemical elements were normalized to the average concentrations of elements in the river waters of western Siberia to estimate the enrichment relative to the regional background (RB, Shvartsev et al. 1996). The concentrations of Zn and Cd in the dump at the processing plant were higher than those in the RB and background concentrations by 2–3 orders of magnitude (sample D-11, Table 2). In the Darasun River, after merging with the technogenic flow (D-15), their concentrations were higher than in the RB and background indicators. The concentration of Pb was higher than that of the RB at the background point, in the drainage flow, and in the Darasun River downstream of the drainage discharge. Tl was found in all of the

studied samples. Its concentration was six times higher than the background value in the Darasun River after merging with the technogenic stream (D-15). The acidic waters of the dump at the processing plant (pH 3.6) contained $1.4 \mu\text{g/L}$ of Be, which was three orders of magnitude higher than the background value (Table 2). The Darasun River downstream contained 3–4 times more Be than the background river. These facts indicate the high mobility of Tl and Be, even in a neutral medium.

The concentrations of As and Sb were increased compared to the RB in all of the technogenic watercourses, especially in the pH 8.9 water of the old hydraulic dump, similar to gold and silver (D-11, Table 2), significantly exceeding the background in the Darasun River downstream after the tailings (D-15, Table 2).

The concentrations of Ag and Au in the settling pond significantly exceeded the background level (sample D-3, Table 2), and in the old settling pond, the concentration of Au in the solution was $130 \mu\text{g/L}$, which was four orders of magnitude greater than the background concentration (sample D-11, Table 2). The enrichment ratios (ERs) of dissolved gold in the Darasun River basin water were calculated and visualized as anomaly maps (Fig. 6):

$$\text{ER} = \frac{C_{\text{Au}}}{\text{background concentration}_{\text{Au}}}, \quad (8)$$

where C_{Au} is the concentration of dissolved Au in water, ng/L and $\text{background concentration}_{\text{Au}}$ —is the average concentration of Au in background river waters (5 ng/L), according to Table 2.

Elevated Au concentrations were found in all of the studied samples, but the concentration in the Darasun River

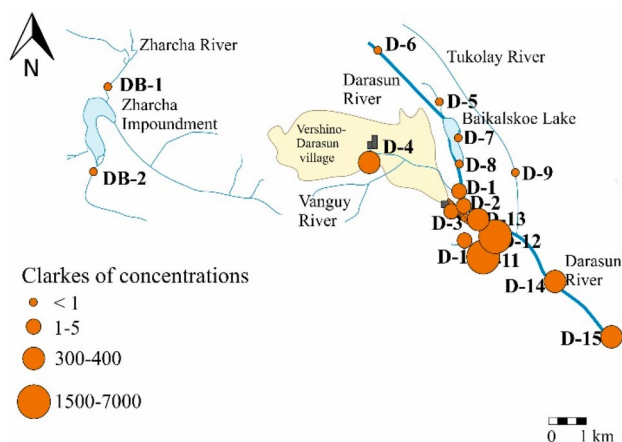


Fig. 6 Clarke concentrations (CC) of dissolved Au in mine drainages (D-1 ÷ D-4), technological ponds (D-11 ÷ D-13), Darasun River catchment before (D-6 ÷ D-8, D-10) and after mine drainage discharge (pp. D-14 ÷ D-15), background points (DB-1 ÷ DB-2)

downstream after the technogenic system (2.3 µg/L) was 460 times greater than the background (Fig. 6). The migration of Au, in this case, was due to the removal of dissolved forms with process water and drainage from places where cyanide waste was stored and complexation with cyanide anions.

The concentrations of total As and cyanide ions in the studied waters were compared with the maximum allowable concentrations of chemicals in drinking and domestic waters (GN 2.1.2.1315-03 2017) and provided as maps of hydrochemical anomalies (Fig. 7).

Conclusions

1. Active hypercryogenic transformation, sulfide oxidation, leaching of chemical elements, and the formation of highly mineralized sulfate and cyanide solutions have occurred in the abandoned Darasun mine tailings. Washed, oxidized horizons were characterized by high electrical resistivities. Geochemical barriers with high metal concentrations were in the “thin” moist layers with

low resistivity. The processes of acid formation in the seasonally-thawed layer are assumed to have been accelerated by the freezing–thawing effect on the underlying frozen horizons, which eventually led to the leaching of a wide range of elements and their dissolution. The thawing zone was well visualized as a region of low electrical resistivities; therefore, ERT could be used in the future to monitor the dynamics of the transformation of the deeper horizons of the tailings body.

- The drainages from the Darasun mine tailings are highly mineralized, acidic, sulfate solutions with high concentrations of cyanide anions, and contain a wide range of metals and metalloids. When it enters natural streams, some of the chemical compounds are precipitated due to acid neutralization and hydrolysis.
- According to their migration ability, elements in surface watercourses were divided into three geochemical associations: (1) ore metals and associated impurities (Tl, Be, In), the mobility of which is controlled by the acidity of the medium. Where the drainage water is diluted by natural waters, the pH value increases, causing Fe, Mn, and Al hydroxides to precipitate, which sorbs other elements, causing their concentrations to decrease. (2) The noble metals (Ag, Au) and metalloids (As, Sb) retain mobility in neutral and subalkaline conditions and migrate, mainly as complex compounds with CN⁻, SO₄²⁻, Cl⁻, and HCO₃⁻ ligands. The mobility of the post-transition metals and metalloids (Bi–Sn–Te) is not related to the acidity of the medium or the concentration of complexing agents, and migration occurs at neutral pH.
- The combined action of two factors, oxidation by air and the dissolved oxygen in water, as well as complexation with cyanide anions, favours the transition from waste to solution and migration with water flows of a whole range of elements, including elements of the 1st hazard class (Tl, Be), and cyanide anions at distances of tens of kilometres from the stored waste.

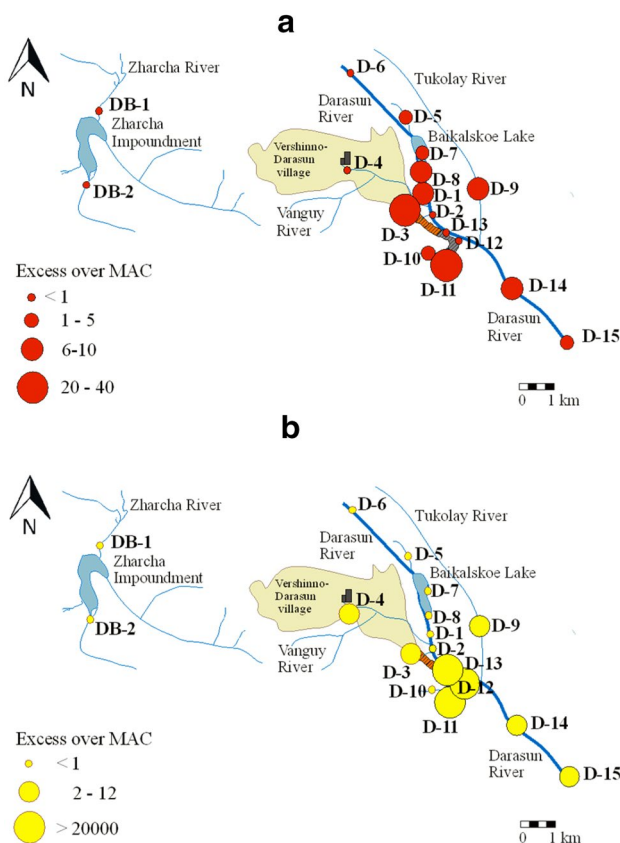


Fig. 7 Enrichment over maximum allowable concentration (GN 2.1.5.1315-03 2017) for dissolved As (a) and CN⁻ (b) in mine drainages (D-1 ÷ D-4), technological ponds (D-11 ÷ D-13), Darasun River catchment before (D-6 ÷ D-8, D-10) and after mine drainage discharge (pp. D-14 ÷ D-15), background points (DB-1 ÷ DB-2)

Supplementary Information The online version contains supplementary material available at <https://doi.org/10.1007/s10230-021-00828-5>.

Acknowledgements This work was supported by the Russian Foundation for Basic Research, Grant 20-05-00336 (laboratory investigations, calculations, visualisation) and Russian Science Foundation, Grant 19-17-00134 (interpretation, conceptualisation).

References

Acero P, Cama J, Ayora C (2007) Rate law for galena dissolution in acidic environment. *Chem Geol* 245:219–229. <https://doi.org/10.1016/j.chemgeo.2007.08.003>

- Acosta JA, Martínez-Pagán P, Martínez-Martínez S, Faz A, Zornoza R, Carmona DM (2014) Assessment of environmental risk of reclaimed mining ponds using geophysics and geochemical techniques. *J Geochem Explor* 147:80–90. <https://doi.org/10.1016/j.gexplo.2014.04.005>
- Albert S, Kvennefors C, Jacob K, Kera J, Grinham A (2017) Environmental change in a modified catchment downstream of a gold mine, Solomon Islands. *Environ Pollut* 231:942–953. <https://doi.org/10.1016/j.envpol.2017.08.113>
- Allan RJ, Hornbrook EW (1970) Development of geochemical techniques in permafrost, Coppermine River region. *Can Min J* 91(4):45–48
- Baena OJR, Aristizábal G, Pimentel MS, Flórez CA, Argumedo CE (2020) Waste management and the elimination of mercury in tailings from artisanal and small-scale gold mining in the Andes municipality of Antioquia. *Colombia Mine Water Environ*. <https://doi.org/10.1007/s10230-020-00728-0>
- Ball JW, Nordstrom DK (1991) WATEQ4F—User's manual with revised thermodynamic data base and test cases for calculating speciation of major, trace and redox elements in natural waters, US Geological Survey, Menlo Park, CA
- Bortnikova S, Olenchenko V, Gaskova O, Yurkevich N, Abrosimova N, Shevko E, Edelev A, Korneeva T, Provornaya I, Eder L (2018) Characterization of a gold extraction plant environment in assessing the hazardous nature of accumulated wastes (Kemerovo region, Russia). *Appl Geochem* 93:145–157. <https://doi.org/10.1016/j.apgeochem.2018.04.009>
- Bortnikova S, Yurkevich N, Devyatova A, Saeva O, Shuvaeva O, Makas A, Troshkov M, Abrosimova N, Kirillov M, Korneeva T, Kremleva T, Fefilov N, Shigabaeva G (2019) Mechanisms of low-temperature vapor-gas streams formation from sulfide mine waste. *Sci Total Environ* 647:411–419. <https://doi.org/10.1016/j.scitotenv.2018.08.024>
- Breuer PL, Hewitt DM, Meakin RL (2008) Does pre-oxidation or lead (II) addition reduce the impact of iron sulfides in cyanidation? In: Young CA, Taylor PR, Anderson CG, Choi Y (eds) Proceedings of symposium of the hydrometallurgy. Soc for Mining, Metallurgy and Exploration Inc, Littleton, pp 750–757
- Carvalho PCS, Neiva AMR, Silva MMVG, Santos ACT (2017) Human health risks in an old gold mining area with circum-neutral drainage, central Portugal. *Environ Geochem Health* 39:43–62. <https://doi.org/10.1007/s10653-016-9806-4>
- Davé NK, Blanchette M (1999) Role of cold climatic conditions in management of reactive mining waste. In: Udd JE, Keen AJ (eds) Mining in the Arctic. Balkema, Rotterdam, pp 115–123
- Dold B, Fontboté L (2001) Element cycling and secondary mineralogy in porphyry copper tailings as a function of climate, primary mineralogy, and mineral processing. *J Geochem Explor* 74:3–55. [https://doi.org/10.1016/S0375-6742\(01\)00174-1](https://doi.org/10.1016/S0375-6742(01)00174-1)
- Epov MI, Yurkevich NV, Bortnikova SB, Karin YG, Saeva OP (2017) Analysis of mine waste by geochemical and geophysical methods (a case study of the mine tailing dump of the Salair ore-processing plant). *Russ Geol Geophys* 58:1543–1552. <https://doi.org/10.1016/j.rgg.2017.11.014>
- Gao S, Jin H, Bense VF, Wang X, Chai X (2019) Application of electrical resistivity tomography for delineating permafrost hydrogeology in the headwater area of Yellow River on Qinghai-Tibet Plateau, SW China. *Hydrogeol J* 27(5):1725–1737. <https://doi.org/10.1007/s10040-019-01942-z>
- Ghasemi S, Mohammadnejad S, Khalesi MR (2018) A DFT study on the speciation of aqueous gold and copper cyanide complexes. *Comput Theor Chem* 1124:23–31. <https://doi.org/10.1016/j.comptc.2017.12.004>
- GN 2.1.5.1315-03 (2017) Maximum allowable concentration (MAC) of chemicals in water of drinking water and cultural and domestic water use. Ministry of Justice, Russian Federation
- Gustafsson JP (2014) Visual MINTEQ 3.1, KTH Royal Institute of Technology. Dept of Land and Water Resource Engineering, Stockholm
- Hawkins AB (2014) Implications of pyrite oxidation for engineering works. Springer International Publishing, Berlin
- Hayley K, Bentley LR, Gharibi M, Nightingale M (2007) Low temperature dependence of electrical resistivity: Implications for near surface geophysical monitoring. *Geophys Res Lett*. <https://doi.org/10.1029/2007GL031124>
- Herring T, Cey E, Pidlisecky A (2019) Electrical resistivity of a partially saturated porous medium at subzero temperatures. *Vadose Zone J* 18:1–11. <https://doi.org/10.2136/vzj2019.02.0019>
- Hudson-Edwards KA, Jamieson HE, Lottermoser BG (2011) Mine wastes: past, present, future. *Elements* 7:375–380. <https://doi.org/10.2113/gselements.7.6.375>
- Khamkhash A, Srivastava V, Ghosh T et al (2017) Mining-related selenium contamination in Alaska, and the state of current knowledge. *Minerals* 7:46. <https://doi.org/10.3390/min7030046>
- Kneisel C, Rödder T, Schwindt D (2014) Frozen ground dynamics resolved by multi-year and yearround electrical resistivity monitoring at three alpine sites in the Swiss Alps. In: near surface geophysics. Editors: Robert Supper, Jonathan Chambers, Panos Tsourlos and Jung-Ho Kim. EAGE Publishing BV, Volume 12, Issue 1, pp 117–132. <https://www.earthdoc.org/content/journals/10.3997/1873-0604.2013068>
- Krautblatter M, Verleysdonk S, Flores-Orozco A, Kemna A (2010) Temperature-calibrated imaging of seasonal changes in permafrost rock walls by quantitative electrical resistivity tomography (Zugspitze, German/Austrian Alps). *J Geophys Res*. <https://doi.org/10.1029/2008JF001209>
- Kvon DA, Modin IN, Shevnev VA, Makarov DV, Skobelev AD (2019) Electrical resistivity tomography, petrophysical modelling, saline permafrost, cooled ground. *Earth's Cryosphere* 23(3):3–10. [https://doi.org/10.21782/EC2541-9994-2019-3\(3-10\)](https://doi.org/10.21782/EC2541-9994-2019-3(3-10))
- Laperdina TG (2002) Estimation of mercury and other heavy metal contamination in traditional gold-mining areas of Transbaikalia. *Geochem Explor Environ A* 2(3):219–223. <https://doi.org/10.1144/1467-787302-025>
- Little AJ, Sivarajah B, Frendo C et al (2020) The impacts of century-old, arsenic-rich mine tailings on multi-trophic level biological assemblages in lakes from Cobalt (Ontario, Canada). *Sci Total Environ* 709:136212. <https://doi.org/10.1016/j.scitotenv.2019.136212>
- Loke MH (2003) Res2dinv-2D resistivity and IP inversion, Geotomo Software, Malaysia
- Lortzie K, Stylianou M, Dermatas D, Kostarelos K (2015) Long-term environmental impact at an abandoned gold–silver enrichment plant: a case study in Mitsero, Cyprus. *Eng Geol* 184:119–125. <https://doi.org/10.1016/j.enggeo.2014.11.011>
- Luque-Almagro VM, Moreno-Vivián C, Roldán MD (2016) Biodegradation of cyanide wastes from mining and jewellery industries. *Curr Opin Biotechnol* 38:9–13. <https://doi.org/10.1016/j.cobio.2015.12.004>
- Marsden J, House I (2006) The chemistry of gold extraction, 2nd edn. Soc for Mining, Metallurgy, and Exploration, Englewood, pp 251–260
- Martín-Crespo T, Gómez-Ortiz D, Martín-Velázquez S, Martínez-Pagán P, de Ignacio-San JC, Lillo J, Faz Á (2020) Abandoned mine tailings affecting riverbed sediments in the Cartagena-La Unión District, Mediterranean coastal area (Spain). *Remote Sens-Basel* 12(12):2042. <https://doi.org/10.3390/rs12122042>
- Mudroch A, Clair TA (1986) Transport of arsenic and mercury from gold mining activities through an aquatic system. *Sci Total Environ* 57:205–216. [https://doi.org/10.1016/0048-9697\(86\)90024-0](https://doi.org/10.1016/0048-9697(86)90024-0)

- Myagkaya IN, Lazareva EV, Gustaytis MA, Zhmodik SM (2016) Gold and silver in a system of sulfide tailings. Part 1: Migration in water flow. *J Geochem Explor* 160:16–30. <https://doi.org/10.1016/j.jgeochem.2015.10.004>
- Nikonow W, Rammlmair D, Furche M (2019) A multidisciplinary approach considering geochemical reorganization and internal structure of tailings impoundments for metal exploration. *Appl Geochem* 104:51–59. <https://doi.org/10.1016/j.apgeochem.2019.03.014>
- Njinga RL, Tshivhase VM (2017) The impact of mine tailings on the Witwatersrand and the surrounding water bodies in Gauteng Province, South Africa. *Mine Water Environ* 36(4):638–645. <https://doi.org/10.1007/s10230-017-0469-x>
- Nordstrom DK (2011) Mine waters: acidic to circumneutral. *Elements* 7:393–398. <https://doi.org/10.2113/gselements.7.6.393>
- Nordstrom DK, Blowes DW, Ptacek CJ (2015) Hydrogeochemistry and microbiology of mine drainage: an update. *Appl Geochem* 57:3–16. <https://doi.org/10.1016/j.apgeochem.2015.02.008>
- Oldenborger GA, LeBlanc AM (2018) Monitoring changes in unfrozen water content with electrical resistivity surveys in cold continuous permafrost. *Geophys J Int* 215:965–977. <https://doi.org/10.1093/GJI/GGY321>
- Olenchenko VV, Kucher DO, Bortnikova SB, Gas'kova OL, Edelev AV, Gora MP (2016) Vertical and lateral spreading of highly mineralized acid drainage solutions (Ur dump, Salair): electrical resistivity tomography and hydrogeochemical data. *Russ Geol Geophys* 57:617–628. <https://doi.org/10.1016/j.rgg.2015.05.014>
- Parbhakar-Fox A (2016) Geoenvironmental characterisation of heap leach materials at abandoned mines: croydon Au-Mines, QLD, Australia. *Minerals* 6:52. <https://doi.org/10.3390/min6020052>
- Parbhakar-Fox A, Lottermoser BG (2015) A critical review of acid rock drainage prediction methods and practices. *Miner Eng* 82:107–124. <https://doi.org/10.1016/j.mineng.2015.03.015>
- Rudnick RL, Gao S (2003) Composition of the continental crust. In: Rudnick R (ed) *The crust*, vol 3. Elsevier, New York
- Saryg-ool BY, Myagkaya IN, Kirichenko IS, Gustaytis MA, Shuvaeva OV, Zhmodik SM, Lazareva EV (2017) Redistribution of elements between wastes and organic-bearing material in the dispersion train of gold-bearing sulfide tailings: part I. geochemistry and mineralogy. *Sci Total Environ* 581–582:460–471. <https://doi.org/10.1016/j.scitotenv.2016.12.154>
- Shvartsev SL, Savichev OG, Vertman GG, Zarubina RF, Nalivaiko NG, Trifonova NG, Turov YuP, Frizen LF, Yankovsky VI (1996) Ecological and geochemical state of river waters in Central Siberia. *Water Resour* 23(6):723–731
- Sinclair SA, Pham N, Amos RT et al (2015) Influence of freeze–thaw dynamics on internal geochemical evolution of low sulfide waste rock. *Appl Geochem* 61:160–174. <https://doi.org/10.1016/j.apgeochem.2015.05.017>
- Sobek AA, Schuller WA, Freeman JR, Smith RM (1978) Field and laboratory methods applicable to overburdens and minesoils, US Environmental Protection Agency, Cincinnati, OH
- Straskraba V, Moran RE (1990) Environmental occurrence and impacts of arsenic at gold mining sites in the western United States. *Int J Mine Water* 9:181–191. <https://doi.org/10.1007/BF02503691>
- U.S. EPA (Environmental Protection Agency) (1994) Treatment of Cyanide Heap Leaches and Tailings. <https://archive.epa.gov/epawaste/nonhaz/industrial/special/web/pdf/cyanide.pdf>. Accessed 30 May 2020
- Williams PJ (1964) Unfrozen water content of frozen soils and soil moisture suction. *Géotechnique* 14:231–246. <https://doi.org/10.1680/geot.1964.14.3.231>
- Woffenden M, Noller B, Noonan K, Breuer P, Cooper P, Donato D (2008) Cyanide management: leading practice sustainable development program for the mining industry. Australian Govt Dept of Resources, Energy and Tourism
- Yurkevich NV, Saeva OP, Pal'chik NA, (2012) Arsenic mobility in two mine tailings drainage systems and its removal from solution by natural geochemical barriers. *Appl Geochem* 27:2260–2270. <https://doi.org/10.1016/j.apgeochem.2012.05.012>
- Yurkevich NV, Saeva OP, Karin YG (2015) Geochemical anomalies in two sulfide-bearing waste disposal areas: Fe, Cu, Zn, Cd, Pb, and As in contaminated waters and snow, Kemerovo and Chelyabinsk regions, Russia. *Toxicol Environ Chem* 97:76–89. <https://doi.org/10.1080/02772248.2015.1041955>
- Yurkevich NV, Abrosimova NA, Bortnikova SB, Karin YG, Saeva OP (2017) Geophysical investigations for evaluation of environmental pollution in a mine tailings area. *Toxicol Environ Chem* 99:1328–1345. <https://doi.org/10.1080/02772248.2017.1371308>
- Yurkevich N, Bortnikova S, Abrosimova N, Makas A, Olenchenko V, Yurkevich N, Edelev A, Saeva O, Shevko A (2019) Sulfur and nitrogen gases in the vapor streams from ore cyanidation wastes at a sharply continental climate, western Siberia, Russia. *Water Air Soil Pollut* 230:307. <https://doi.org/10.1007/s11270-019-4363-y>